

Enhanced field emission from hexagonal rhodium nanostructures

Bhaskar R. Sathe, Bhalchandra A. Kakade, Imtiaz S. Mulla, Vijayamohanan K. Pillai, Dattatray J. Late, Mahendra A. More, and Dilip S. Joag

Citation: [Applied Physics Letters](#) **92**, 253106 (2008); doi: 10.1063/1.2943657

View online: <http://dx.doi.org/10.1063/1.2943657>

View Table of Contents: <http://scitation.aip.org/content/aip/journal/apl/92/25?ver=pdfcov>

Published by the [AIP Publishing](#)

Articles you may be interested in

[Enhanced field emission properties from well-aligned zinc oxide nanoneedles grown on the Au/Ti/n - Si substrate](#)

Appl. Phys. Lett. **90**, 083107 (2007); 10.1063/1.2643979

[Field emission of one-dimensional micro- and nanostructures of zinc oxide](#)

Appl. Phys. Lett. **89**, 043108 (2006); 10.1063/1.2234838

[Enhanced electron field emission from oriented columnar AlN and mechanism](#)

Appl. Phys. Lett. **88**, 251103 (2006); 10.1063/1.2216353

[Electron field emission from GaN nanorod films grown on Si substrates with native silicon oxides](#)

Appl. Phys. Lett. **86**, 082109 (2005); 10.1063/1.1869549

[Preparation and characterization of nanostructured film of graphitized diamond crystallites for field electron emission](#)

J. Appl. Phys. **94**, 5429 (2003); 10.1063/1.1611281

The advertisement features a 3D cutaway simulation of a mechanical part with a red-to-blue color gradient. The text 'Over 600 Multiphysics Simulation Projects' is prominently displayed in white and blue. A blue button with the text 'VIEW NOW >>' is located in the bottom right corner. The COMSOL logo is positioned at the bottom right of the image.

Over **600** Multiphysics Simulation Projects

[VIEW NOW >>](#)

COMSOL

Enhanced field emission from hexagonal rhodium nanostructures

Bhaskar R. Sathe,¹ Bhalchandra A. Kakade,¹ Imtiaz S. Mulla,¹ Vijayamohan K. Pillai,^{1,a)} Dattatray J. Late,² Mahendra A. More,² and Dilip S. Joag²

¹Physical and Materials Chemistry Division, National Chemical Laboratory, Pune 411 008, India

²Department of Physics, University of Pune, Pune 411 007, India

(Received 5 March 2008; accepted 19 May 2008; published online 25 June 2008)

Shape selective synthesis of nanostructured Rh hexagons has been demonstrated with the help of a modified chemical vapor deposition using rhodium acetate. An ultralow threshold field of $0.72 \text{ V}/\mu\text{m}$ is observed to generate a field emission current density of $4 \times 10^{-3} \mu\text{A}/\text{cm}^2$. The high enhancement factor (9325) indicates that the origin of electron emission is from nanostructured features. The smaller size of emitting area, excellent current density, and stability over a period of more than 3 h are promising characteristics for the development of electron sources. © 2008 American Institute of Physics. [DOI: 10.1063/1.2943657]

Metal nanoparticles of tunable size and shape have been the central focus of current research due to their exotic electronic, optical, and magnetic properties that are often different from their bulk counterparts.^{1–3} The manipulation of the electronic structure of these materials at the nanoscale has strong implications on the development of high-throughput electronic devices, such as those based on field emission. Field emission from nanostructured materials in particular has captured extensive attention in the past few years due to the enormous field enhancement possible at sharp tips anticipated as a function of size and shape in the nanoscale; in addition to normal criteria for the choice of materials such as low resistivity, high refractivity, and structural anisotropy.^{4–6} Consequently, a number of anisotropic materials have been found to act as an efficient field emission cathodes, since some of these can operate remarkably well below the intrinsic current limit due to their thermal effects.⁵ Enormous improvements have been made, to date, in metal nanostructures using ruthenium (Ru), platinum (Pt), palladium (Pd), rhodium (Rh), rhenium (Re), and iridium (Ir), since most of these have their work function comparable to that of silicon.^{7,8} Among these, Rh could especially be promising due to its features such as excellent electrical performance, chemical inertness, mechanical strength, remarkable thermal stability, lower electron affinity, and significant stability toward ion bombardment.^{9,10} Although the work function of Rh is higher by $\sim 100\text{--}200 \text{ meV}$ than that of metals such as Pt and Re,⁸ their anisotropic nanostructures by virtue of sharp tips could facilitate enhanced field emission. Here, we report such an enhanced field emission from hexagonal Rh nanostructures synthesized using a modified chemical vapor deposition.

Synthesis of these Rh hexagonal nanostructures briefly involves heating rhodium acetate precursor at $950 \text{ }^\circ\text{C}$ on alumina substrate at $5 \text{ }^\circ\text{C}/\text{min}$ in presence of argon flowing at 250 sccm (sccm denotes standard cubic centimeter per minute at STP); more details are similar to our previous report.¹¹ The use of this type of a precursor with Rh–Rh bond (having a dimeric structure) is indispensable for the growth of hexagons, since rhodium chloride, rhodium nitrate, etc., do not generate such a remarkable morphology.

Figure 1(a) shows a typical scanning electron microscopy (SEM) image of Rh hexagons synthesized at $950 \text{ }^\circ\text{C}$ suggesting a high yield along with uniform features. A high density of coalesced Rh hexagons having an edge length of $\sim 5\text{--}6 \mu\text{m}$ with a monodispersed (edge size) thickness of $\sim 300 \text{ nm}$ at the central edge could be clearly seen in Fig. 1(b). These hexagons are described as nanostructured since their dimensions at the tip/edge are in nanoregime as revealed by the transmission electron microscopy (TEM) image Fig. 1(d) (responsible for their enhanced field emission), despite having their length in microns. The unique morphological features when compared to other regular hexagons include their central thicker edge and sharper pointed tip of $\sim 100 \text{ nm}$. Moreover from Fig. 1(c), electron dispersive X-ray (EDX) analysis confirms the local chemical composition, where peaks at 2.68 and 2.89 keV could be identified as the $L\beta_1$ and $L\alpha_1$ emission X-ray signals of Rh respectively. The signal at 0.68 keV corresponds to carbon of highly oriented pyrolytic graphite substrate. These findings are in excellent agreement with the data obtained by X-ray diffraction (XRD) analysis [Fig. 2(a)], where the presence of five promi-

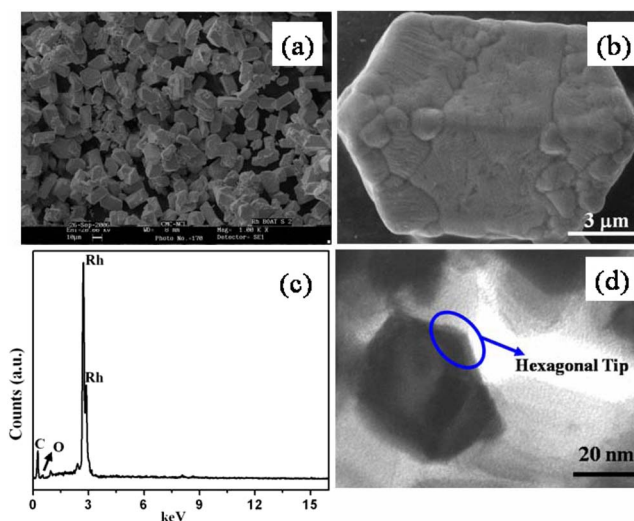


FIG. 1. (Color online) (a) SEM image of as synthesized Rh hexagonal structures along with (b) an image of high magnification. (c) Elemental composition as obtained from spot EDX and (d) TEM image of single hexagons with highlighted sharp tips of 10 nm .

a) Author to whom correspondence should be addressed. Electronic mail: vk.pillai@ncl.res.in. FAX: +91-20-25882636.

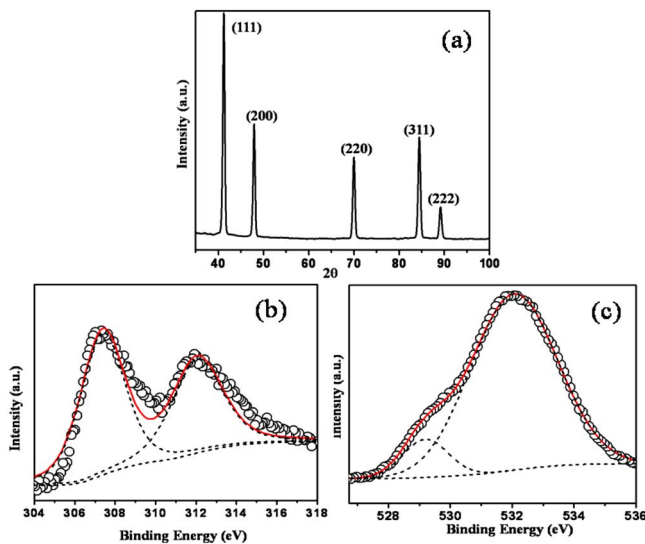


FIG. 2. (Color online) (a) XRD pattern of Rh hexagons revealing reflections from the (111), (200), (220), (311), and (222) planes along with XP spectra corresponding to (b) Rh and (c) oxygen, respectively.

nent fcc reflections corresponding to the (111), (200), (220), (311), and (222) planes suggest the single phase nature of Rh(0). Moreover, X-ray photoelectron spectra corresponding to Rh3d and O1s also help to explain the predominance of Rh(0) peak with perhaps, a minimum amount of unavoidable surface oxide as clearly seen [Figs. 2(b) and 2(c)].

Field emission measurements were carried out in a conventional microscopic tube evacuated at a base pressure 1×10^{-9} mbar with interesting features. The cathode (nanostructured Rh hexagons deposited on a silicon substrate) was held at a distance ~ 10 mm from the transparent anode screen in a vacuum chamber. Accordingly, Fig. 3(a) shows typical emission current density-applied field characteristics for the diode configuration, where an onset field of $0.6 \text{ V}/\mu\text{m}$, requiring an emission current of 1 nA (corresponding to the current density of $4 \times 10^{-3} \mu\text{A}/\text{cm}^2$) is reproducibly observed. With the increase in the applied field, the emission current density increases very rapidly, finally reaching $40 \mu\text{A}/\text{cm}^2$ at $1.76 \text{ V}/\mu\text{m}$. This could be compared with the recent results on metallic tungsten nanowires, where an applied field of $5 \text{ V}/\mu\text{m}$ generates an emission current density of $0.1 \text{ mA}/\text{cm}^2$, which is important for many applications.¹²

Figure 3(b) shows Fowler–Nordheim plot, where a straight line behavior indicates that the emission from the Rh hexagons follows a quantum mechanical tunneling process, similar to that reported for metallic emitters. The applied electric field (F) is defined as $F = V/d$, where V is the voltage

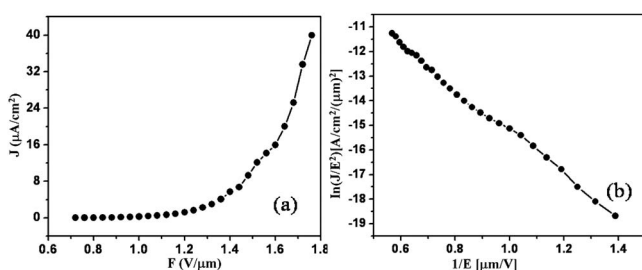


FIG. 3. Field emission (a) J - F characteristics and (b) Fowler–Nordheim plot for Rh hexagons/Si showing typical metallic behavior of the emitter.

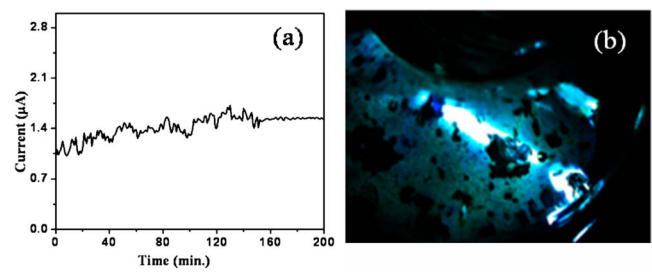


FIG. 4. (Color online) (a) I - t transients of Rh hexagons along with its (b) field emission micrograph. Bright spots on the screen represent emission at an applied potential of 10 kV from the protrusions on the emitter surface.

and d is the separation ($d = 5 \text{ mm}$). However, the actual enhanced field at the apex of the hexagons can be estimated from the equation as follows:¹³

$$\beta = -6.8 \times 10^3 \phi^{3/2}/m, \quad (1)$$

where β is field enhancement factor and ϕ is the work function of the emitter material in eV. The field enhancement factor β is calculated to be 9325 (by taking the work function of Rh as 5.25 eV on HfO_2 substrate⁸) and this high value of β is attributed to the presence of nanoscale protrusions on the edges/tips (surface heterogeneity), as seen in Fig. 1(b), which could be responsible for lowering the threshold leading to a final increase in the resultant current. Chen *et al.* have reported a similar enhancement due to nanoprotuberances on amorphous diamond films.¹⁴ In comparison, our hexagons are much bigger in size and the areal density is about 100 times smaller (10^6 cm^{-2} compared to 10^8 cm^{-2}) perhaps, due to the use of single crystalline Si substrates.

Field emission current stability is one of the decisive parameters in the context of practical applications of cold cathodes. The field emission current stability of Rh/Si has been investigated at a preset current of $1 \mu\text{A}$ (corresponding to the current density of $4 \times 10^{-3} \mu\text{A}/\text{cm}^2$), over duration of more than 3 h. Accordingly, Fig. 4(a) shows the current-time (I - t) plot for this preset current value at a base pressure of 1×10^{-9} mbar. Significantly, our Rh hexagons exhibit a remarkable current stability for repeated performance without any obvious signs of degradation, making an initial excursion to $\sim 1.5 \mu\text{A}$. Further, a good current stability with current fluctuations within about $\pm 15\%$ of the average value is seen over a period of more than 3 h as also confirmed by repetitive measurement of I - t transients. The observed current fluctuations in the form of spikes could be attributed to adsorption/desorption of the residual gas molecules at the grain boundaries on the emitter surface. Moreover, self-diffusion of atoms at the tip in the presence of high electric field is also expected to contribute to these fluctuations. The observed field emission pattern comprises of bright and symmetric oval shaped spots having higher image stability, as revealed in Fig. 4(b). Table I shows a comparison of the field emission properties of common nanostructures along with corresponding synthetic methods to highlight the importance of the low threshold for our Rh hexagons. Interestingly, the surface morphology of the Rh hexagons on Si substrate by SEM after the field emission measurements shows no severe deterioration even after a long-term operation of the emitter. This signifies that the Rh hexagons are mechanically robust and have strong resistance toward ion bombardment during the electron emission.

TABLE I. Comparison of the field-emission performance of some recently reported nanostructures with that of our Rh hexagons.

Sr. No.	Emitter Nanostructures	Synthesis method	Turn-on field	Field-enhancement factor (β)	Current Stability	Ref.
1	ZnO Nanowires	Vapor phase growth	6 V/ μm at 0.1 $\mu\text{A}/\text{cm}^2$	847	2h	15
2	Ge cone arrays	Electron beam evaporation	15 V/ μm at 1 mA	560	...	16
3	SnO ₂ nanorods	Thermal evaporation method	2.3–4.5 V/ μm at 1 $\mu\text{A}/\text{cm}^2$	1796	2h	17
4	Rh hexagons	Chemical vapor deposition	0.72 V/ μm at $4 \times 10^{-3} \mu\text{A}/\text{cm}^2$	9325	≥ 3 h	Present studies
5	AlN nanotips	Chemical vapor deposition	10.8 V/ μm at 10 mA/ cm^2	367 and 317	...	18
6	Strontium oxide coated CNTs	Magnetron sputter deposition	4.4 V/ μm at 1.96 mA/ cm^2	467	...	19

In summary, we report the synthesis of nanostructured Rh hexagons along with their remarkable field emission behavior. The presence of sharp tips (100 nm) of the nanopositions with an areal density of $10^6/\text{cm}^2$ is believed to be responsible for a stable current density of 40 $\mu\text{A}/\text{cm}^2$ that is drawn from the emitter at 1.76 V/ μm along with their excellent current and mechanical stability toward ions bombardment.

B.R.S. thank Council of Scientific and Industrial Research for financial support.

¹V. Colvin, M. Schlamp, and A. Alivisatos, *Nature (London)* **370**, 354 (1994).

²W. de Heer, A. Chatelain, and D. Ugarte, *Science* **270**, 1179 (1995).

³T. Ahmadi, Z. Wang, T. Green, A. Henglein, and M. El-Sayed, *Science* **272**, 1924 (1996).

⁴C. Masarapu, J. Ok, and B. Wei, *J. Phys. Chem. C* **111**, 12112 (2007).

⁵X. Fang, Y. Bando, U. Gautam, C. Ye, and D. Golberg, *J. Mater. Chem.* **18**, 509 (2008).

⁶N. Ramgir, I. Mulla, K. Vijayamohan, D. Late, A. Bhise, M. More, and D. Joag, *Appl. Phys. Lett.* **88**, 042107 (2006).

⁷S. Day, J. Goswami, D. Gu, H. Waard, S. Marcus, and C. Werkhoven, *Appl. Phys. Lett.* **84**, 1606 (2004).

⁸K. Park and G. Parsons, *Appl. Phys. Lett.* **89**, 043111 (2006).

⁹F. A. Cotton and G. Wilkinson, *Advance Inorganic Chemistry*, 4th ed. (Wiley, New York, 1980).

¹⁰S. W. Rosencrance, J. S. Burnham, D. E. Sanders, C. He, B. J. Garrison, N. Winograd, Z. Postawa, and A. E. De Pristo, *Phys. Rev. B* **52**, 6006 (1995).

¹¹N. Ramgir, I. Mulla, and K. Vijayamohan, *J. Phys. Chem. B* **108**, 14815 (2004).

¹²S. Kim, J. Baik, H. Yu, K. Kim, Y. Tak, and J. Lee, *Appl. Phys. Lett.* **18**, 072105 (2005).

¹³R. Fowler and L. Nordheim, *Proc. R. Soc. London, Ser. A* **119**, 173 (1928).

¹⁴J. Chen, S. Deng, J. Chen, N. Xu, and S. Huq, *Appl. Phys. Lett.* **80**, 4030 (2002).

¹⁵C. Lee, T. Lee, S. Lyu, Y. Zhang, H. Ruh, and H. Lee, *Appl. Phys. Lett.* **81**, 3648 (2004).

¹⁶Q. Wan, T. Wang, T. Feng, X. Liu, and C. Lin, *Appl. Phys. Lett.* **81**, 3281 (2002).

¹⁷L. Zhao, Q. Pang, Y. Cai, N. Wang, W. Ge, J. Wang, and S. Yang, *J. Phys. D: Appl. Phys.* **40**, 3587 (2007).

¹⁸Z. Chen, C. Cao, and H. Zhu, *J. Phys. Chem. C* **111**, 1895 (2007).

¹⁹F. Jin, Y. Liu, C. Day, and S. Little, *Carbon* **45**, 587 (2007).